Fundamental Journal of Mathematics and Applications, 7(3) (2024), 147-157

Research Paper / Open Access

Fundamental Journal of Mathematics and Applications

ISSN Online: 2645-8845

www.dergipark.org.tr/en/pub/fujma

https://doi.org/10.33401/fujma.1524621

Investigation of Power-Law Fluid on a Decelerated Rotating Disk

Serkan Ayan [1,†,*] **and Burhan Alveroğlu** [1,‡]

[1] *Bursa Technical University, Faculty of Science and Engineering, Department of Mathematics, Bursa, Türkiye*

[†] *serkan.ayan@btu.edu.tr*, [‡] *burhan.alveroglu@btu.edu.tr*

[*] *Corresponding Author*

Article Information

Keywords: Decelerated rotating disk flows; Boundary layer analysis; Similarity solutions; Non-newtonian fluids

AMS 2020 Classification: 76E07; 76U05

Abstract

This study explores the behaviour of power-law fluids over decelerating rotating disks. The disk's angular velocity decreases inversely with time, and the unsteady governing equations modeling this flow yield similarity transformations that depend on the nondimensional parameter $\hat{\alpha} = \frac{\alpha}{\Omega_0}$. These transformations, introduced here for the first time in the literature, allow for a comprehensive analysis of the fluid dynamics for shear-thinning fluids within the range $0.5 < n \leq 1$.

We examine the no-slip boundary condition alongside the dimensionless unsteadiness parameter, which quantifies the initial deceleration or acceleration of the disk. We present velocity profiles and the viscosity function for various values of $\hat{\alpha}$. The boundary layer problem, formulated through dimensionless momentum and continuity equations derived via similarity transformations, is solved using the `bvp4c` function in MATLAB. This numerical method, employing the 4th-order Runge-Kutta algorithm, provides approximate solutions for the U, V, and W velocity profiles and the μ viscosity function, considering different deceleration parameters and the power-law index n.

Our findings contribute novel insights into the fluid dynamics of power-law fluids in decelerating rotational systems, offering potential applications in industrial and engineering processes where such conditions are prevalent.

1. Introduction

The study of boundary layer analysis on rotating disks has been a topic of significant interest in fluid dynamics research. This area was first explored by Theodore von Karman [1], who established the foundational equations for steady boundary layer flow. The von Kármán boundary layer flow is part of a broader family of flow types characterized by the differential rotation rate between a solid disk and an incompressible fluid rotating above it as a rigid body. This family of flows is known as BEK system flows [2]. The groundbreaking experimental analysis using the china-clay technique conducted by Gregory and Stuart [3] revealed a notable similarity between the von Kármán rotating-disk flow and flows over swept wings. This work demonstrated that despite the apparent differences between these two flow configurations, they exhibit comparable flow patterns and boundary layer characteristics. This discovery prompted the investigation of rotating disk flow as a prototypical case for both empirical and theoretical research.

The von Kármán rotating-disk flow has indeed become a fundamental model for analyzing the transition from laminar to turbulent flow in three-dimensional boundary layers. This model has been widely applied across various scenarios involving rotating disks due to its simplicity and the rich insights it provides into flow behaviour.

Malik's pioneering numerical study [4], together with Lingwood's investigations [5, 6, 7] and more recent contributions like Appelquist's theoretical work [8], have greatly advanced our understanding of steady flows over smooth rotating disks. These theoretical studies have explored various aspects of the flow, including the stability of laminar boundary layers and the mechanisms leading to turbulence, thereby advancing our knowledge of the transition processes in such flows.

Studies on rotating flows with rough disks have also significantly advanced the understanding of boundary layer dynamics. Notably, research by Harris et al. [9] investigated the effects of surface roughness on the flow characteristics over rotating disks, revealing how roughness influences the transition to turbulence and changes the base flow profiles. Cooper and Carpenter

Received: 30-07-2024 **Revised:** 17-09-2024 **Accepted:** 20-09-2024 **Online:** 27-09-2024 **Published:** 30-09-2024

[10] further explored these effects, focusing on theoretical aspects of how rough surfaces modify boundary layer behaviour. Additionally, Cooper et al. [11] examined the impact of various types of surface roughness on rotating disk flows, contributing to a broader understanding of how surface imperfections affect flow transition and turbulence. Further insights are provided by studies such as those by Alveroglu and Christian [12, 13], which offer valuable perspectives on the complex interactions between surface roughness and rotating flow dynamics.

Although the studies mentioned above primarily focus on Newtonian fluids, significant progress has been made in extending the von Kármán boundary layer flow analysis to non-Newtonian fluids. Mitschka [14] was pivotal in this extension, utilizing a boundary layer approximation to explore how non-Newtonian behaviours influence the flow characteristics around rotating disks. This work marked a significant shift from classical Newtonian models, offering new insights into the behaviour of fluids with complex viscosity profiles. After that, both Mitschka and Ulbrecht [15] as well as Andersson et al. [16] and Hussain et al. [17] contributed valuable numerical solutions for the basic flow in the context of shear-thickening and shear-thinning fluids. Mitschka and Ulbrecht focused on the numerical analysis of shear-thinning and shear-thickening fluids, which exhibit an increase in viscosity with increasing shear rate, while Andersson et al. examined highly shear-thickening fluids. Their work has provided a deeper understanding of how these non-Newtonian properties affect the flow dynamics around rotating disks, revealing differences in boundary layer behaviour and flow transition characteristics compared to Newtonian fluids. These studies have expanded the applicability of von Kármán's work, making it relevant for a broader range of industrial and scientific applications where non-Newtonian fluids are present. However, Denier and Hewit [18] investigated the problem for both shear-thinning and shear-thickening fluids and showed that there are some fundamental issues regarding the application of power-law models in the boundary layer context. More recently, instability analysis examined in the boundary layer of rotating disks for shear-thinning fluids [19, 20, 21]. Using a sixth-order linear stability equation system, they found that increasing shear thinning stabilizes type I and type II modes in the flow. The results are consistent with established asymptotic estimates and provide new insights into the critical Reynolds number and growth rate. In [22], power-law fluids was conducted by Abdulameer et al., investigating the effect of shear-thinning fluids on convective type I and type II instability modes was analyzed using the Chebyshev polynomial method. Further, Alqarni et al. [23] have demonstrated, the local linear convective instability of boundary-layer flows over rough rotating disks using the Carreau model, a different type of non-Newtonian flow, by determining steady-flow profiles. It has been also shown by Lingwood and Henrik Alfredsson [24] that the rotating disk boundary layer itself exhibits a large number of complex instability behaviours that are not yet fully understood.

In addition to these studies, the decelerated rotating disk case investigated viscous flow and emphasised the relationship between fluid stresses and velocities [25, 26]. Further, Turkyılmazoglu et al. [27] focused on the heat transfer characteristics in nanofluid MHD flow across a decelerated rotating disk with uniform suction, and also the impact of uniform suction and magnetohydrodynamics on several nanofluids, such as silver, alumina, and copper, were studied Rahman et al. [28] over a decelerated rotating disk. Additionally, Fang and Tao [29] studied the laminar unsteady flow across a stretchy decelerated rotating disk. These works contributed to the growing body of knowledge on how velocity changes affect fluid behaviour on decelerating rotating disks.

In particular, the similarity transformations of non-Newtonian fluids and the related velocity profiles and viscosity functions are discussed, focusing on the shear-thinning states and the dimensionless unsteadiness parameter of these fluids. This way, the similarity transformations for power-law fluids are obtained on a decelerating rotating disk and solved numerically using MATLAB's bvp4c function. This function's numerical approach relies on a finite difference code that implements the three-stage Lobatto IIIa formula, equivalent to an implicit Runge-Kutta formula with a continuous interpolant [30].

This research examines a non-Newtonian fluid with non-constant viscosity contained in a container and rotates non-uniformly with an angular velocity that varies with time (t) in an inertial frame. The equation of motion for a fluid element about a reference frame may be found using the conservation of momentum concept. The mathematical description of rotating fluids may be done using a variety of reference frames. Adopting a reference frame whose axes are fixed in a fluid-filled container is physically and mathematically natural for many geophysical problems, such as atmospheric dynamics. This is often referred to as a rotating frame, mantle frame, or body frame so that the bounding surface of the container is constant and there are only minor deviations from rigid body rotation [31].

2. Formulation

We consider the steady incompressible power-law fluid reviews that geometry is an infinite rotating plane, stating at $z^* = 0$ and also we use the symbol * to indicate the dimensional parameter. However, since we use the assumption that the disk is decelerating, we consider the inertial frame. The plane rotates with a angular velocity $\Omega_D^* = \Omega_0(1-\alpha t^*)^{-1}$, decelerating around $z^* = 0$. The continuity and Navier-Stokes equations can be considered as

$$\boldsymbol{\nabla}\cdot\boldsymbol{u}^* = 0 \tag{2.1}$$

$$\frac{\partial \boldsymbol{u}^*}{\partial t^*} + \boldsymbol{u}^*\cdot\nabla\boldsymbol{u}^* + 2\boldsymbol{\Omega}_{\boldsymbol{D}}^*\times\boldsymbol{u}^* + \boldsymbol{r}\times\left(\frac{\partial \boldsymbol{\Omega}_{\boldsymbol{D}}}{\partial t^*}\right) = -\frac{1}{\rho^*}\nabla p^* + \frac{1}{\rho^*}\boldsymbol{\nabla}\cdot\boldsymbol{\tau}^*. \tag{2.2}$$

Here U^*, V^*, W^* are the steady velocity components in cylindrical polar coordinates, $\boldsymbol{r} = (r^*, \theta, z^*)$ is the position vector, t^* is

the time and $\mathbf{\Omega}_D^* = (0,0,\Omega_D^*)$ is the vector form of the angular velocity of the disk that describes the disk just rotates about the z^* axis with angular velocity Ω_D^*. Moreover, ρ^* is the fluid density and p^* is the pressure. The stress tensor $\boldsymbol{\tau}^*$ for generalised Newtonian models, is defined by

$$\boldsymbol{\tau}^* = \mu^* \dot{\boldsymbol{\gamma}}^* \quad \text{with} \quad \mu^* = \mu^*(\dot{\gamma}^*)$$

where $\dot{\boldsymbol{\gamma}}^* = \boldsymbol{\nabla} \boldsymbol{u}^* + (\boldsymbol{\nabla} \boldsymbol{u}^*)^T$ is the rate-of-strain tensor and $\mu^*(\dot{\gamma}^*)$ is the non-Newtonian viscosity. The magnitude of the symmetric rate-of-strain tensor is given by

$$\dot{\gamma}^* = \sqrt{\frac{\dot{\boldsymbol{\gamma}}^* : \dot{\boldsymbol{\gamma}}^*}{2}}.$$

The Navier Stokes Equations written for incompressible fluids together with the inertial frame for the reference whose axes rotate in a container filled with fluid are as follows,

$$\frac{1}{r^*}\frac{\partial (r^* U_0^*)}{\partial r^*} + \frac{1}{r^*}\frac{\partial V_0^*}{\partial \theta} + \frac{\partial W_0^*}{\partial z^*} = 0 \tag{2.3}$$

$$\frac{\partial U_0^*}{\partial t^*} + U_0^*\frac{\partial U_0^*}{\partial r^*} + \frac{V_0^*}{r^*}\frac{\partial U_0^*}{\partial \theta} + W_0^*\frac{\partial U_0^*}{\partial z^*} - \frac{(V_0^* + r^*\Omega^*)^2}{r^*} = \frac{1}{\rho^*}\frac{\partial}{\partial z^*}\left(\mu^*\frac{\partial U_0^*}{\partial z^*}\right), \tag{2.4}$$

$$\frac{\partial V_0^*}{\partial t^*} + U_0^*\frac{\partial V_0^*}{\partial r^*} + \frac{V_0^*}{r^*}\frac{\partial V_0^*}{\partial \theta} + W_0^*\frac{\partial V_0^*}{\partial z^*} + \frac{U_0^*\widetilde{V}_0^*}{r^*} + 2\Omega^* U_0^* + r^*\frac{\partial \Omega^*}{\partial t^*} = \frac{1}{\rho^*}\frac{\partial}{\partial z^*}\left(\mu^*\frac{\partial V_0^*}{\partial z^*}\right), \tag{2.5}$$

$$\begin{aligned}&\frac{\partial W_0^*}{\partial t^*} + U_0^*\frac{\partial W_0^*}{\partial r^*} + \frac{V_0^*}{r^*}\frac{\partial W_0^*}{\partial \theta} + W_0^*\frac{\partial W_0^*}{\partial z^*}\\ &= -\frac{1}{\rho^*}\frac{\partial P_1^*}{\partial z^*} + \frac{1}{\rho^* r^*}\frac{\partial}{\partial r^*}\left(\mu^* r^*\frac{\partial U_0^*}{\partial z^*}\right) + \frac{1}{\rho^* r^*}\frac{\partial}{\partial \theta}\left(\mu^*\frac{\partial V_0^*}{\partial z^*}\right) + \frac{2}{\rho^*}\frac{\partial}{\partial z^*}\left(\mu^*\frac{\partial W_0^*}{\partial z^*}\right).\end{aligned} \tag{2.6}$$

Here U_0^*, $,V_0^*$, W_0^* are the leading order velocity components and P_1^* is the leading order pressure term. The rate-of-strain tensor $\dot{\gamma}^*$ can be written to be

$$\begin{aligned}\dot{\gamma}^* = \sqrt{\frac{II}{2}} \quad = \quad &\left\{2\left[\left(\frac{\partial U^*}{\partial r^*}\right)^2 + \left(\frac{1}{r^*}\frac{\partial V^*}{\partial \theta} + \frac{U^*}{r^*}\right)^2 + \left(\frac{\partial W^*}{\partial z^*}\right)^2\right]\right.\\ &\left. + \left[r^*\frac{\partial}{\partial r^*}\left(\frac{V^*}{r^*}\right) + \frac{1}{r^*}\frac{\partial U^*}{\partial \theta}\right]^2 + \left(\frac{\partial U^*}{\partial z^*} + \frac{\partial W^*}{\partial r^*}\right)^2 + \left(\frac{\partial V^*}{\partial z^*} + \frac{1}{r^*}\frac{\partial W^*}{\partial \theta}\right)^2\right\}^{1/2}\end{aligned} \tag{2.7}$$

where

$$II = \sum_i \sum_j \dot{\gamma}_{ij}^{*2} = \dot{\gamma}_{r^*r^*}^{*2} + \dot{\gamma}_{\theta\theta}^{*2} + \dot{\gamma}_{z^*z^*}^{*2} + 2\left(\dot{\gamma}_{r^*\theta}^{*2} + \dot{\gamma}_{r^*z^*}^{*2} + \dot{\gamma}_{\theta z^*}^{*2}\right).$$

To determine the unsteady mean flow relative to the disk, we offer the generalization of the standard Newtonian similarity solution. So, we consider the following transformations,

$$U_0^* = U(\eta) r^* \Omega_D^*,\ V_0^* = V(\eta) r^* \Omega_D^*,\ W_0^* = W(\eta)\chi^*,\ P_1^* = \rho^* \chi^{*^2}, \tag{2.8}$$

where

$$\chi^* = \left[\frac{\nu^*}{r^{*^{1-n}}(\Omega_0(1-\alpha t^*)^{-1})^{1-2n}}\right]^{1/(n+1)}.$$

Here U, V, W are the dimensionless radial, azimuthal and axial base flow velocities, respectively. Additionally, P is the pressure and $\nu^* = \frac{m^*}{\rho^*}$ is the kinematic viscosity. The dimensionless similarity coordinate that can be also named as boundary layer thickness is

$$\eta = \frac{r^{*\frac{1-n}{n+1}} z^*}{L^{*^{2/(n+1)}}},\ \text{where } L^* = \sqrt{\frac{\nu^*}{(\Omega_0(1-\alpha t^*)^{-1})^{2-n}}}.$$

These similarity variables account for the time-dependent variation of boundary layer thickness and represent the first instance of such an introduction for power-law fluids in the literature.
Consequently, the similarity equations for the governing boundary layer equations of a decelerated power-law fluid, represented by equations (2.1) and (2.2), are derived for the first time as follows:

$$2U + \frac{1-n}{1+n}\eta U' + W' = 0$$

$$\begin{aligned}
&\hat{\alpha}\left(U-\frac{n-2}{n+1}\eta U'\right)+U^2+\left(\eta\frac{1-n}{n+1}U+W\right)U'-(V+1)^2-(\mu U')'=0,\\
&\hat{\alpha}\left(V-\frac{n-2}{n+1}\eta V'+1\right)+V'\left(\eta\frac{1-n}{n+1}U+W\right)+2U(V+1)-(\mu V')'=0,\\
&\hat{\alpha}\left(\frac{2n-1}{n+1}W+\frac{2-n}{n+1}\eta W'\right)+\frac{1-n}{n+1}\left[U\left(\eta W'-V\right)+2\mu U'\right]+2\mu' U+P'+WW'-(\mu W')'=0.
\end{aligned} \tag{2.9}$$

where the primes denote differentiation with respect to η and the viscosity function is

$$\mu=\left[U'^2+V'^2\right]^{\frac{n-1}{2}}.$$

Owing to (2.9) the non-dimensional boundary conditions are

$$U(0)=V(0)=W(0)=0, U(\eta\to\infty)\to 0 \text{ and } V(\eta\to\infty)\to -1. \tag{2.10}$$

To obtain the flow profiles U, V and W, the dimensionless mean flow equations (2.9) valid for the power-law are expressed as a system of first order ordinary differential equations. This system of equations is written as five coupled first order equations in terms of the new five dependent variables $\psi_n(n=1,2,...,5)$, which are defined as follows:

$$\psi_1=U,\ \psi_2=U',\ \psi_3=V,\ \psi_4=V',\ \psi_5=W. \tag{2.11}$$

Using the first order equations defined by (2.11), the transformed system of first order ordinary differential equations with no-slip boundary conditions for power-law fluids is obtained as follows:

$$\begin{aligned}
\psi_1' &= \psi_2\\
\psi_2' &= \frac{(\psi_2^2+n\psi_4^2)f-\psi_2\psi_4(n-1)g}{n\mu(\psi_2^2+\psi_4^2)}\\
\psi_3' &= \psi_4\\
\psi_4' &= \frac{(n\psi_2^2+\psi_4^2)g-\psi_2\psi_4(n-1)f}{n\mu(\psi_2^2+\psi_4^2)}\\
\psi_5' &= -2\psi_1-\frac{1-n}{1+n}\eta\psi_2.
\end{aligned} \tag{2.12}$$

The nondimensional boundary conditions are

$$\begin{aligned}
&\psi_1(0)=\psi_3(0)=\psi(0)=0\\
&\psi_1(\infty)\to 0,\ \psi_3(\infty)\to -1.
\end{aligned} \tag{2.13}$$

Also in (2.12), f and g are given below

$$\begin{aligned}
f &= \hat{\alpha}(u-(n-2)/(n+1)\eta\psi_2)+\psi_1^2-(\psi_3+1)^2+(\psi_5+\hat{\psi}\psi_1)\psi_2,\\
g &= \hat{\alpha}(\psi_3-(n-2)/(n+1)\eta\psi_4+1)+2\psi_1(\psi_3+1)+(\psi_5+\hat{\psi}\psi_1)\psi_4,
\end{aligned}$$

with $\hat{\psi}=(1-n)/(1+n)\eta$. These equations simplify to the Newtonian case when $n=1$, aligning with established literature. Although these equations are applicable to both shear-thickening ($n>1$) and shear-thinning ($n<1$) fluids, Denier and Hewitt [18] demonstrated that bounded solutions of (2.9) subject to (2.10) exist only for shear-thinning fluids with $n>0.5$. Consequently, Griffits et al. [19, 22] investigated power-law indexed flows within the range $0.5<n\leq 1$ for a steady rotating flow. In line with their work, this study also focuses on shear-thinning fluids with $0.5<n\leq 1$ in the context of a decelerated rotating disk.

3. Results and Discussion

The obtained similarity equations (2.9) were solved approximately in MATLAB using the bvp4c function in accordance with the boundary conditions given in (2.10) and the following velocity profiles were obtained. Hussain et al. [17] expanded the range of $\hat{\alpha}$ to -100, building upon earlier work by Watson and Wang [25], who established that a disk can only have a momentum layer if it is decelerating, i.e., when $\hat{\alpha}<0$. Rahman et al. [28] later provided numerical solutions for eight different values of $\hat{\alpha}$ in the interval $0\leq -\hat{\alpha}\leq 20$. Here, by choosing $0.5<n\leq 1$, we observe that the flow is non-Newtonian and we observe the changes due to the unsteadiness parameter $0\leq -\hat{\alpha}\leq 8$. The unsteadiness parameter was truncated at $\hat{\alpha}=-8$ because of the discrepancies in the results obtained due to the deceleration of the rotating disk.

Before performing the calculations, the numerical scheme needed to be validated using a comparison methodology. Table 2 presents a comparison with the results of [25, 29] the classical Newtonian fluid case. The compared data are in good agreement, which not only validates the code but also demonstrates the accuracy and reliability of the numerical scheme.

$n = 0.6$

$\hat{\alpha}$	$U'(0)$	$V'(0)$	$W(\infty)$
0	0.5	−0.6770	−1.3046
−0.5	0.5416	−0.4858	−0.8241
−2	0.5011	−0.0785	−0.3312
−5	0.3515	−0.2152	−0.0948
−8	0.2783	−0.3293	−0.0430

$n = 0.7$

$U'(0)$	$V'(0)$	$W(\infty)$
0.5015	−0.6530	−1.1967
0.5638	−0.4676	−0.8391
0.6433	−0.0050	−0.4438
0.6637	0.6416	−0.1846
0.6191	1.0941	−0.0989

$n = 0.8$

$\hat{\alpha}$	$U'(0)$	$V'(0)$	$W(\infty)$
0	0.5039	−0.6362	−1.0773
−0.5	0.5826	−0.4523	−0.8436
−2	0.7633	0.0610	−0.5660
−5	1.0053	1.0296	−0.3399
−8	1.1075	1.9083	−0.2331

$n = 0.9$

$U'(0)$	$V'(0)$	$W(\infty)$
0.5069	−0.6243	−0.9688
0.5992	−0.4394	−0.8469
0.8583	0.1141	−0.6923
1.3165	1.2624	−0.5516
1.6824	2.4214	−0.4715

$n = 1$

$\hat{\alpha}$	$U'(0)$	$V'(0)$	$W(\infty)$
0	0.5102	−0.6159	−0.8845
−0.5	0.6143	−0.4284	−0.8510
−2	0.9315	0.1550	−0.8193
−5	1.5628	1.3609	−0.8012
−8	2.1873	2.5887	−0.7941

Table 1: Table of boundary values for U, V and W

$n = 1$

$\hat{\alpha} = -0.5$	[25]	[29]	Present
$U'(0)$	0.614283	0.6143	0.6143
$V'(0)$	-0.428406	-0.4284	-0.4284
$W(\infty)$	0.4255		-0.8510

$\hat{\alpha} = -2$	[25]	[29]	Present
$U'(0)$	0.931507	0.9315	0.9315
$V'(0)$	0.154981	0.1550	0.1550
$W(\infty)$	0.4096		-0.8193

$\hat{\alpha} = -5$	[25]	[29]	Present
$U'(0)$	1.562797	1.5627	1.5628
$V'(0)$	1.360850	1.3609	1.3609
$W(\infty)$	0.4006		-0.8012

Table 2: Comparison of $U'(0)$, $V'(0)$ and $W(\infty)$ obtained for various $\hat{\alpha}$ variables with the results of [25] and [29] the classical Newtonian fluid case.

The power-law shear-thinning flow profiles calculated for the decelerating disk are illustrated in Figures 1, 2, and 3. They reveal that all those profiles decay to their corresponding far field values as decelarating parameter decreases. Figure 1 reveals a notable decrease in the boundary layer thickness as the instability parameter $-\hat{\alpha}$ increases. This decrease becomes more pronounced with increasing $-\hat{\alpha}$, ultimately leading to a significant reduction in the boundary layer thickness. Additionally, the

maximum value of the radial jet also decreases as $-\hat{\alpha}$ grows in magnitude. Also, as deceleration increases, the location of the maximum value of the radial jet shifts closer to the disk surface. Despite these changes in boundary layer thickness and radial jet strength, the inflectional shape of the flow profile remains preserved, indicating stability in the overall flow structure.

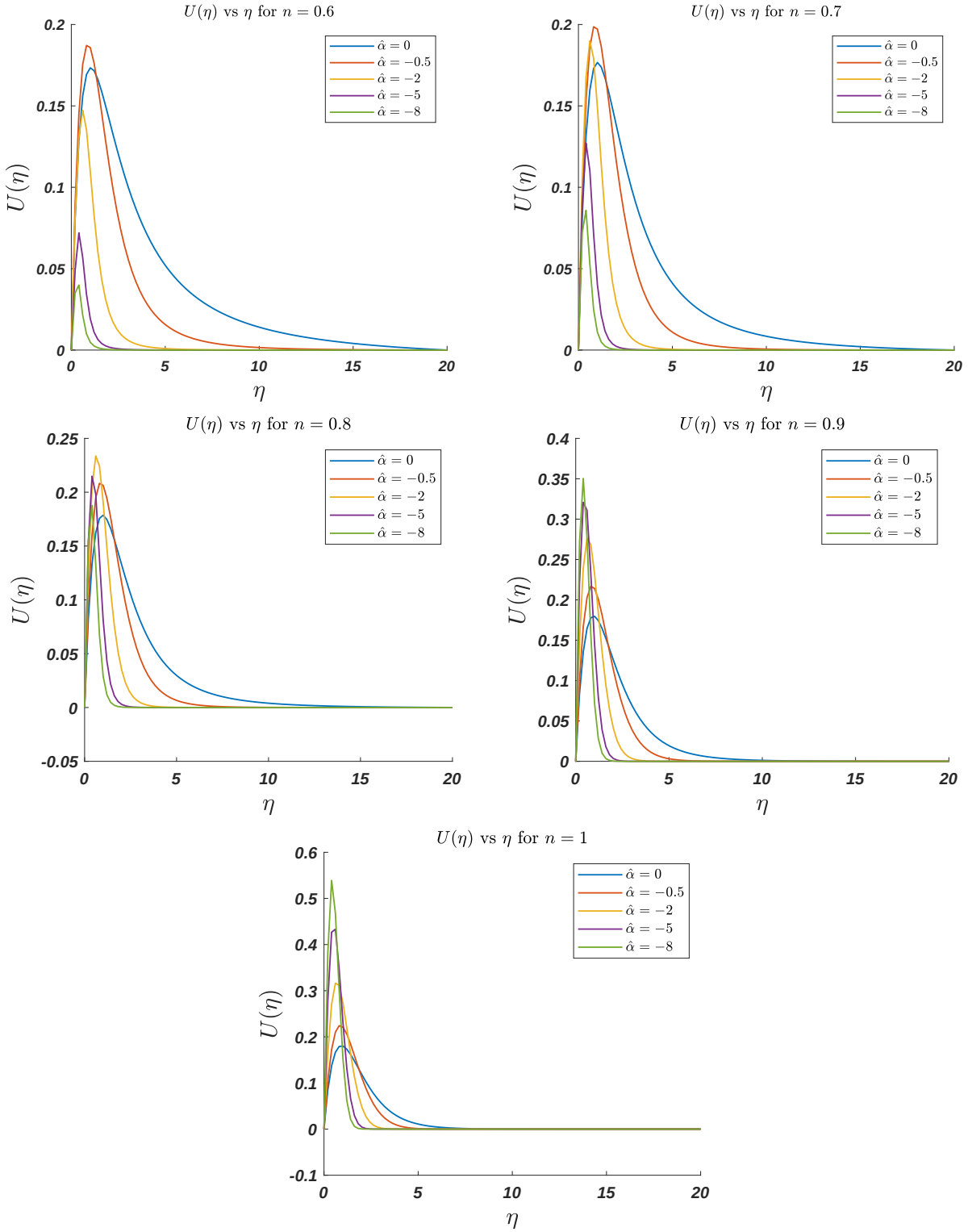

Figure 1: Radial velocity profiles for power-law flow for $0.5 < n \leq 1$ versus η. The boundary layer thickness η axis has been truncated at 20.

The effect of non-zero $\hat{\alpha}$ on the azimuthal profile is presented in Figure 2. For each value of the shear-thickening parameter n, the figure demonstrates that the transition of the profile to the boundary value at the far field becomes more rapid as the disk's deceleration increases. This observation is consistent with the decrease in boundary layer thickness noted previously.

Figure 3 shows the axial velocity profile for various values of the shear-thickening parameter n. The figure illustrates that an

increased deceleration rate leads to a significant reduction in the magnitude of the axial jet, hence reduce the amount of the fluid entering the boundary layer. Furthermore, the decrease in the magnitude of the axial flow becomes more pronounced as the shear-thickening parameter n decreases.

For small unsteadiness parameter values, the fluid ahead of the disk rotates slower than the disk. This phenomenon may be a consequence of the rapid decelerated rotation of the disk, while the inertia of the neighbouring fluid layer allows the fluid to sustain its more significant angular momentum for a long time. Also, as shown in Figures 1, 2, 3 the results are consistent with the boundary layer analysis for a disk rotating at constant velocity ($\hat{\alpha} = 0$). This involves approximate solutions that are directly identical to the result for constant angular velocity rotation of the disk and whose velocity profiles are equivalent to those obtained for flows with known power-law indexes [19].

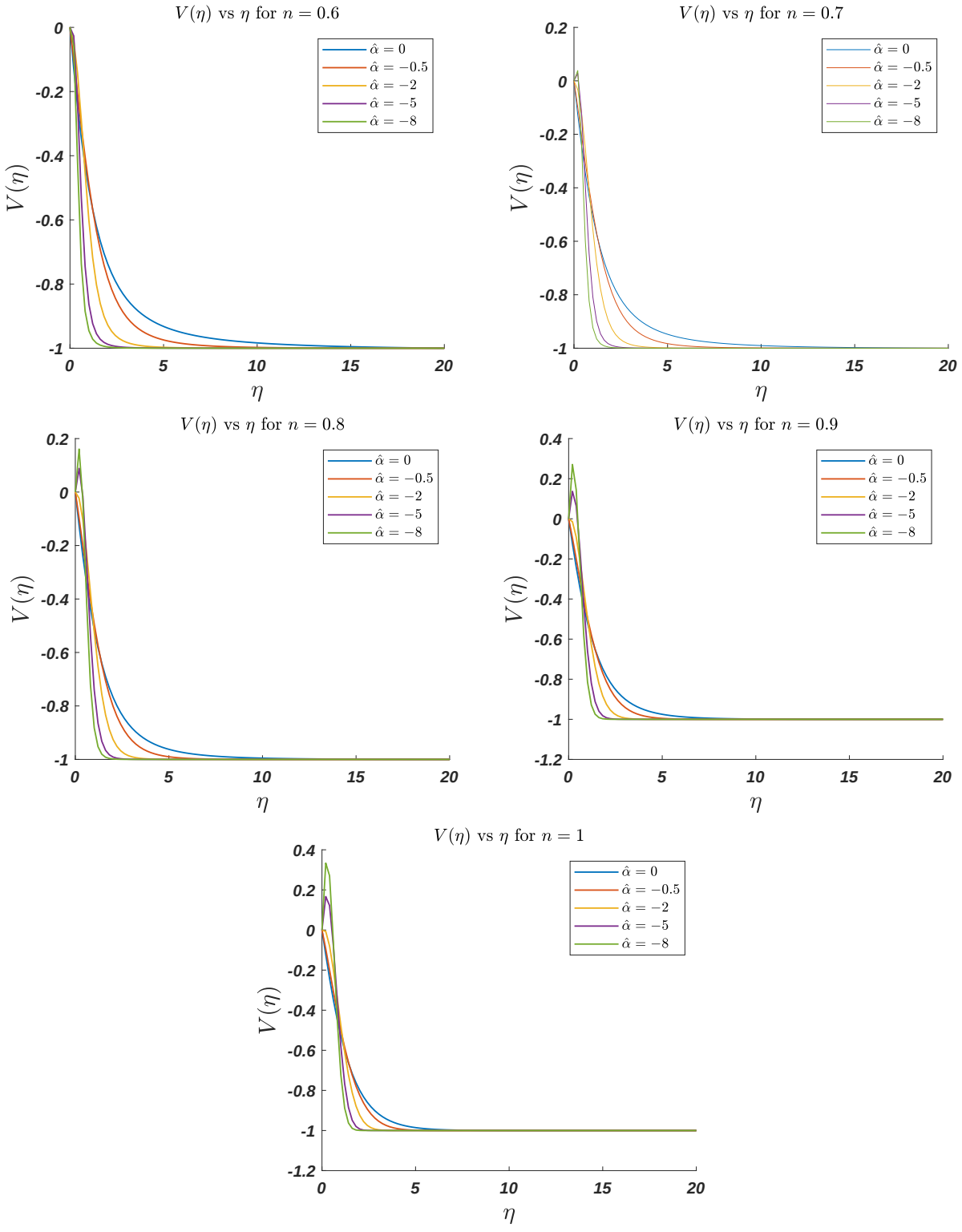

Figure 2: Azimuthal velocity profiles for power-law flow for $0.5 < n \leq 1$ versus η. The boundary layer thickness η axis has been truncated at 20.

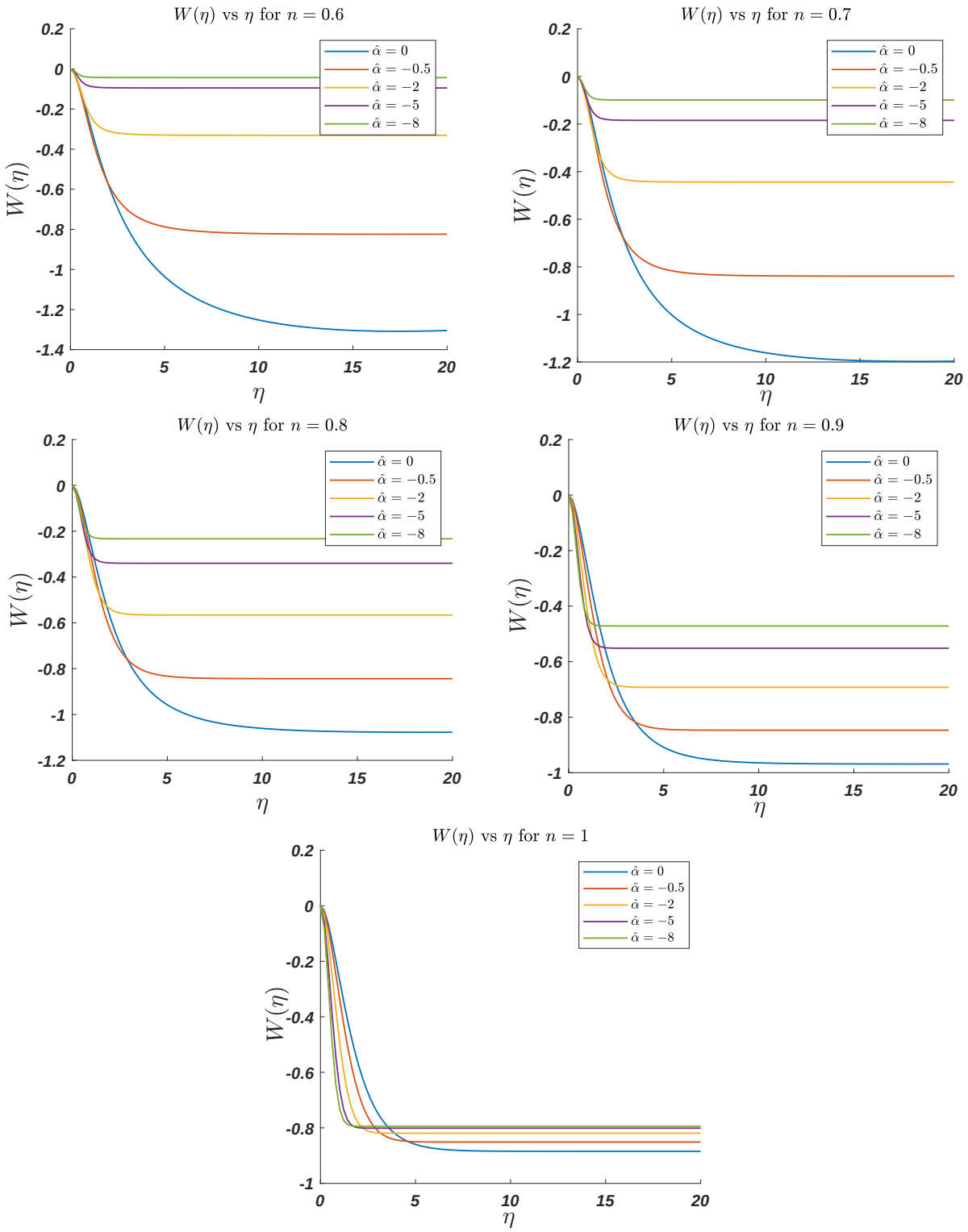

Figure 3: Axial velocity profiles for power-law flow for $0.5 < n \leq 1$ versus η. The boundary layer thickness η axis has been truncated at 20.

Finally, viscosity profiles for the numerical results obtained are given in Figure 4. As the angular velocity of the disk slows down with time, the viscous effects of the flow on the wall surface increase, the numerical data obtained when the power-law index $n = 0.6$ show a decrease by almost half as n increases.

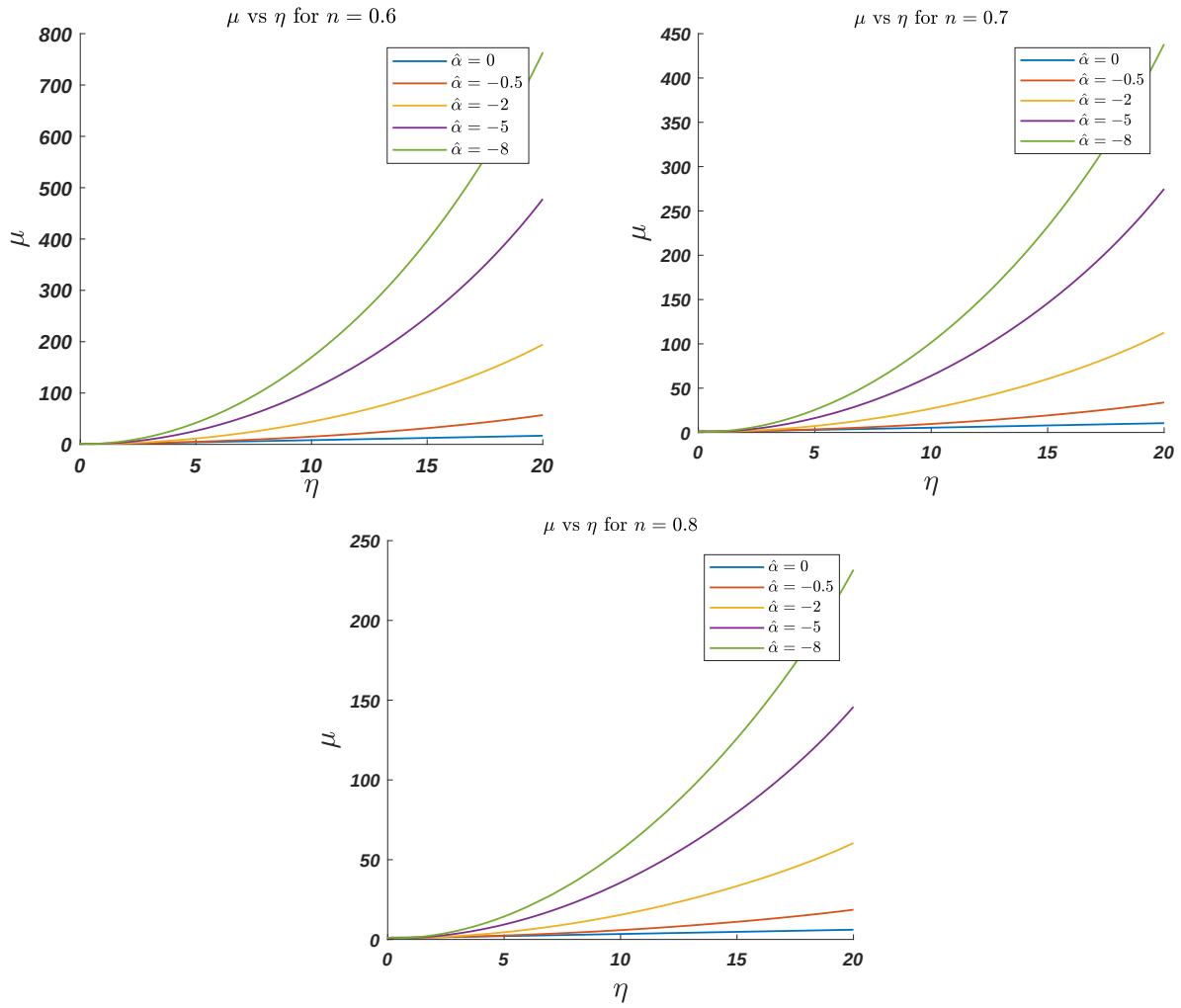

Figure 4: μ versus η for $n = 0.6, 0.7, 0.8$.

4. Conclusion

This study investigates power-law fluids over decelerating rotating disks, with the disk's angular velocity inversely proportional to time. By deriving similarity transformations, we explored the flow characteristics dependent on the nondimensional unsteadiness parameter $\hat{\alpha}$. For $0.5 < n \leq 1$, we analyzed the no-slip condition and the dimensionless unsteadiness parameter, detailing the velocity profiles and viscosity function with respect to deceleration parameters $\hat{\alpha} = 0, -0.5, -2, -5, -8$. The findings revealed that an increased decelerating parameter results in a thinner boundary layer and a reduction in the maximum value of the U profile. It also causes a decrease in the amount of axial flow towards the boundary layer, which is consistent with the observed reduction in boundary layer thickness. Additionally, it was observed that the inflectional profile of mean flow components does not change notably with varying deceleration rates. These findings provide valuable insights into the behaviour of non-Newtonian fluids over decelerating rotating disks, with applications in engineering and industrial processes. The study demonstrates the effectiveness of numerical methods in solving complex fluid dynamics problems, contributing to advancements in the field.

For future work, this study can be extended to include other non-Newtonian fluid models, such as the Bingham and Carreau models, which could offer a more comprehensive understanding of fluid behaviours in different scenarios. Additionally, exploring cases with rough rotating disks could provide insights into how surface texture influences flow dynamics. Finally, it would be valuable to investigate other flow scenarios within the BEK system for non-Newtonian cases. Exploring these different flow configurations could further enhance our understanding of non-Newtonian fluid dynamics and contribute additional insights to the field. Incorporating these elements could enhance the applicability and relevance of our findings. We anticipate that our results will serve as a useful foundation for these extended studies, contributing valuable data and insights to the field.

Declarations

Acknowledgements: The authors are grateful to the anonymous referee for helpful suggestions to improve the paper.

Author's Contributions: Conceptualization, S.A and B.A.; methodology S.A. and B.A.; validation, S.A. and B.A. investiga-

tion, S.A. and B.A.; resources, S.A. and B.A.; data curation, S.A.; writing—original draft preparation, S.A; writing—review and editing, S.A. and B.A.; supervision, B.A. All authors have read and agreed to the published version of the manuscript.

Conflict of Interest Disclosure: The authors declare no conflict of interest.

Copyright Statement: Authors own the copyright of their work published in the journal and their work is published under the CC BY-NC 4.0 license.

Supporting/Supporting Organizations: This research received no external funding.

Ethical Approval and Participant Consent: This article does not contain any studies with human or animal subjects. It is declared that during the preparation process of this study, scientific and ethical principles were followed and all the studies benefited from are stated in the bibliography.

Plagiarism Statement: This article was scanned by the plagiarism program. No plagiarism detected.

Availability of Data and Materials: Data sharing not applicable.

Use of AI tools: The author declares that he has not used Artificial Intelligence (AI) tools in the creation of this article.

ORCID
Serkan Ayan https://orcid.org/0000-0003-3041-2324
Burhan Alveroğlu https://orcid.org/0000-0003-2699-9898

References

[1] T. Von Kármán, *Über laminare und turbulent reibung Z. angew.*, Math und Mech, **1** (1921), 233-52. [CrossRef]
[2] W.G. Cochran, *The flow due to a rotating disc*, Math. Proc. Cambridge Philos. Soc., **30**3 (1934), 365-375. [CrossRef]
[3] N. Gregory, J.T. Stuart, W.S. Walker, *On the stability of three-dimensional boundary layers with application to the flow due to a rotating disk*, Philos. Trans. Roy. Soc. A, **248**(943) (1955), 155-199. [CrossRef]
[4] M.R. Malik, *The neutral curve for stationary disturbances in rotating-disk flow*, J. Fluid Mech., **164** (1986), 275-287. [CrossRef] [Scopus] [Web of Science]
[5] R.J. Lingwood, *Absolute instability of the boundary layer on a rotating disk*, J. Fluid Mech., **299** (1995), 17-33. [CrossRef] [Scopus] [Web of Science]
[6] R.J. Lingwood, *An experimental study of absolute instability of the rotating-disk boundary-layer flow*, J. Fluid Mech., **314** (1996), 373-405. [CrossRef] [Scopus] [Web of Science]
[7] R.J. Lingwood, *Absolute instability of the Ekman layer and related rotating flows*, J. Fluid Mech., **331** (1997), 405-428. [CrossRef] [Scopus] [Web of Science]
[8] E. Appelquist, S. Imayama, P.H. Alfredsson, P. Schlatter and R.J. Lingwood, *Linear disturbances in the rotating-disk flow: a comparison between results from simulations, experiments and theory*, Eur. J. Mech. B Fluids, **55** (2016), 170-181. [CrossRef] [Scopus] [Web of Science]
[9] J. Harris, P. Thomas and S. Garrett, *On the stability of flows over rough rotating disks*, In 42nd AIAA Fluid Dynamics Conference and Exhibit, (2012), 3075. [CrossRef] [Scopus]
[10] A.J. Cooper and P.W. Carpenter, *The stability of rotating-disc boundary-layer flow over a compliant wall. Part 1. Type I and II instabilities*, J. Fluid Mech., **350**(1997), 231-259. [CrossRef] [Scopus] [Web of Science]
[11] A.J. Cooper, J.H. Harris, S.J. Garrett, M. Özkan and P.J. Thomas, *The effect of anisotropic and isotropic roughness on the convective stability of the rotating disk boundary layer*, Phys. Fluids, **27**(1) (2015). [CrossRef] [Web of Science]
[12] B. Alveroglu, A. Segalini and S.J. Garrett, *The effect of surface roughness on the convective instability of the BEK family of boundary-layer flows*, Eur. J. Mech. B Fluids, **56** (2016), 178-187. [CrossRef] [Scopus] [Web of Science]
[13] C. Thomas, B. Alveroğlu, S.O. Stephen, M.A. Al-Malki and Z. Hussain, *Effect of slip on the linear stability of the rotating disk boundary layer*, Phys. Fluids, **35**(8) (2023). [CrossRef] [Scopus] [Web of Science]
[14] P. Mitschka, *Nicht-newtonsche flüssigkeiten ii. drehströmungen ostwald-de waelescher nicht-newtonscher flüssigkeiten*, Collect. Czechoslov. Chem. Commun., **29**(12) (1964), 2892-2905. [CrossRef]
[15] P. Mitschka and J. Ulbrecht, *Nicht-Newtonsche flüssigkeiten IV. Strömung nicht-Newtonscher flüssigkeiten Ostwald-de-Waeleschen typs in der umgebung rotierender drehkegel und scheiben*, Collect. Czechoslov. Chem. Commun., **30**(8) (1965), 2511-2526. [CrossRef]
[16] H.I. Andersson, E. De Korte and R. Meland, *Flow of a power-law fluid over a rotating disk revisited*, Fluid Dyn. Res., **28**(2) (2001), 75. [CrossRef] [Scopus] [Web of Science]
[17] S. Hussain, F. Ahmad, M. Shafique and S. Hussain, *Numerical solution for accelerated rotating disk in a viscous fluid*, Appl. Math., **4**(6) (2013), 899-902. [CrossRef]
[18] J.P. Denier and R.E. Hewitt, *Asymptotic matching constraints for a boundary-layer flow of a power-law fluid*, J. Fluid Mech., **518** (2004), 261–279. [CrossRef] [Scopus] [Web of Science]
[19] P.T. Griffiths, S.J. Garrett and S.O. Stephen, *The neutral curve for stationary disturbances in rotating disk flow for power-law fluids*, J. Non-Newton. Fluid Mech., **213** (2014), 73-81. [CrossRef] [Scopus] [Web of Science]
[20] S.J. Garrett and N. Peake, *The stability and transition of the boundary layer on a rotating sphere*, J. Fluid Mech., **456** (2002), 199-218. [CrossRef] [Scopus] [Web of Science]
[21] R.J. Lingwood and S.J. Garrett, *The effects of surface mass flux on the instability of the BEK system of rotating boundary-layer flows*, Eur. J. Mech. B Fluids, **30**(3) (2011), 299-310. [CrossRef] [Scopus] [Web of Science]
[22] M.A. Abdulameer, P.T. Griffiths, B. Alveroğlu and S.J. Garrett, *On the stability of the BEK family of rotating boundary-layer flows for power-law fluids*, J. Non-Newton. Fluid Mech., **236** (2016), 63-72. [CrossRef] [Scopus] [Web of Science]
[23] A.A. Alqarni, B. Alveroğlu, P.T. Griffiths and S.J. Garrett, *The instability of non-Newtonian boundary-layer flows over rough rotating disks*, J. Non-Newton. Fluid Mech., **273** (2019), 104174. [CrossRef] [Scopus] [Web of Science]
[24] R.J. Lingwood and P. Henrik Alfredsson, *Instabilities of the von Kármán boundary layer*, Appl. Mech. Rev., **67**(3) (2015), 030803. [CrossRef] [Scopus] [Web of Science]
[25] L.T. Watson and C. Wang, *Deceleration of a rotating disk in a viscous fluid*, Phys. Fluids, **22**(12) (1979), 2267-2269. [CrossRef] [Scopus]
[26] A. Majeed, A. Zeeshan, T. Mahmood, S.U. Rahman and I. Khan, *Impact of magnetic field and second-order slip flow of casson liquid with heat transfer subject to suction/injection and convective boundary condition*, J. Magn., **24**(1) (2019), 81-89. [CrossRef] [Scopus] [Web of Science]

[27] M. Rahman, M. Türkyılmazoğlu, M. Bilal and F. Sharif, *On heat transfer with unsteady MHD nanofluid von Karman flow with uniform suction*, Pramana - J. Phys., **97**(4) (2023), 146. [CrossRef] [Scopus] [Web of Science]
[28] M. Rahman, F. Sharif, M. Türkyılmazoğlu and M.S. Siddiqui, *Unsteady three-dimensional magnetohydrodynamics flow of nanofluids over a decelerated rotating disk with uniform suction* Pramana, **96**(4) (2022), 170. [CrossRef] [Scopus] [Web of Science]
[29] T. Fang and H. Tao, *Unsteady viscous flow over a rotating stretchable disk with deceleration*, Commun. Nonlinear Sci. Numer. Simul., **17**(12) (2012), 5064-5072. [CrossRef] [Scopus] [Web of Science]
[30] J. Kierzenka and L.F. Shampine, *A BVP solver based on residual control and the Maltab PSE*, ACM Trans. Math. Softw., **27**(3) (2001), 299-316. [CrossRef] [Scopus] [Web of Science]
[31] K. Zhang and X. Liao, *Theory and modeling of rotating fluids: convection, inertial waves and precession*, Cambridge University Press, (2017).

Fundamental Journal of Mathematics and Applications (FUJMA), (Fundam. J. Math. Appl.)
https://dergipark.org.tr/en/pub/fujma

All open access articles published are distributed under the terms of the CC BY-NC 4.0 license (Creative Commons Attribution-Non-Commercial 4.0 International Public License as currently displayed at http://creativecommons.org/licenses/by-nc/4.0/legalcode) which permits unrestricted use, distribution, and reproduction in any medium, for non-commercial purposes, provided the original work is properly cited.

How to cite this article: S. Ayan and B. Alveroğlu, *Investigation of power-law fluid on a decelerated rotating disk*, Fundam. J. Math. Appl., **7**(3) (2024), 147-157. DOI 10.33401/fujma.1524621